Experiments in Fluids 24 (1998) 375–381 © Springer-Verlag 1998

Combined laser-doppler and cold wire anemometry for turbulent heat flux measurement

D. K. Heist, I. P. Castro

Abstract A combined laser-doppler and cold wire anemometry technique for determining turbulent heat flux is described. The system can be used in flows of arbitrarily high turbulent intensity and large temperature variations. Its potential is demonstrated via measurements in a simulated stable atmospheric boundary layer, for which the Monin-Obukhov length scale was about 70% of the boundary layer depth. Mean and turbulence properties were obtained throughout the boundary layer and the results are shown to be both internally consistent and similar to corresponding field data. Measurements in the highly turbulent, separated flow behind a bluff body mounted in the stable boundary layer are also presented.

1 Introduction

The study of isothermal flows in which (small) temperature sources are used as a surrogate for passive scalars, or of genuinely non-neutral flows in which the temperature and velocity fields are dynamically linked, often involves determination of the turbulent heat flux. This requires simultaneous measurement of velocity and temperature fluctuations, which is classically accomplished with the use of a crossed hot wire in conjunction with a cold wire. There are numerous examples in the literature of the application of this general approach (see, for example, Antonia et al. 1977, 1988; Hishida and Nagano 1979; Gibson and Verriopoulos 1984) although most of these are for essentially neutral flows in which the temperature differences are small. A comprehensive description of appropriate methods is given by Bruun (1995). The cross-wire must be calibrated over a range of temperatures in order to deduce velocity information from the output voltages; such calibration procedures are complex, often taking a few hours to complete (e.g. Lienhard 1988). There are, in addition, other drawbacks to the use of such techniques, the most important of which arise in flows of relatively high turbulence intensities and/or large temperature fluctuations. In the former case, there are well-known inadequacies in hot wire anemometry arising from the limited yaw and pitch response of (particularly) cross-wire probes. In the latter case, obtaining calibrations which allow unambiguous determination of the instantaneous velocities and temperatures can be extremely difficult.

Because of our interest in the simulation of stable and convective atmospheric boundary layers in which (at model scale) mean temperature variations can be as much as 60 °C, and the subsequent study of (sometimes highly turbulent) flows within such boundary layers, a different approach was required. The basic difficulties with the thin-wire techniques arise from the velocity rather than the temperature transducer. By using a system based on a cold-wire anemometer synchronised with a laser Doppler anemometer (LDA), one can substantially reduce the calibration time required, extend the range of turbulence intensities over which the measurements are valid and avoid most of the limitations which arise in cases of large temperature fluctuations. The cold-wire is a simple instrument to calibrate since its voltage output has a linear response to changes in temperature. The LDA needs no calibration and does not suffer from the same limitations as hot wire anemometry as regards yaw response, provided frequency shifting is used to provide directional sensitivity; the difficulties that *can* arise (e.g. from seeding uncertainties, etc) are relatively straightforward to overcome.

There have been a few previous, independent and recent applications of such a technique. Wardana et al. (1995) used an LDA plus cold wire system to study strongly heated channel flows and Pietri et al. (1996) used a similar system to study a slightly heated turbulent jet. Thole and Bogard (1994) described the basic principles of the technique in rather more detail than these authors. This previous work was all in the context of relatively small-scale flows (so that the beam optics could be mounted outside the flows of interest) but was sufficiently encouraging to suggest that the approach could be more widely implemented. In this paper we describe our own LDA-plus-cold-wire synchronised measurement system, whose details differ in some respects from the earlier works, largely in that cooled, fibre-optic probe heads had to be developed because of the large scale and high temperatures of the flows to be studied. The general experimental arrangements are described in the following section, Sect. 3 discusses some aspects of the system in more detail and, in Sect. 4 and as a demonstration of the effectiveness of the technique, we present

Received: 9 May 1997/*Accepted*: 2 September 1997

D. K. Heist, I. P. Castro
School of Mechanical and Materials Engineering
University of Surrey
Guildford, Surrey, GU2 5XH, U.K.

Correspondence to: I. P. Castro

The comments of the authors' colleagues, Alan Robins and Bill Snyder, are gratefully acknowledged, as is the assistance of EnFlo's technical staff in constructing the necessary hardware. DKH was supported by the Natural Environment Research Council throughout the work.

measurements of turbulent heat flux in a stably stratified boundary layer and in a highly turbulent wake. Some implications and conclusions are given in the final section.

2
Experimental set-up

2.1
Anemometry equipment

Both single and two-component LDA systems were used in the present work. The single component measurements were made using a helium neon 50 mW laser giving a 632.8 nm red beam and the two-component system comprised a 5 W argon ion laser with blue and green beams (488 and 514.5 nm respectively). In view of the size of the wind tunnel in which measurements were required (3.5 m in span) a fibre-optic based delivery and receiving system was imperative. The beam splitting, frequency shifting, and coupling of laser light to fibre optic cables were all accomplished using Dantec 60X FiberFlow optics. To eliminate directional ambiguity in measurement of the vertical velocity component, w, (with u and v the axial and spanwise components, respectively) the LDA systems were used in the fringe mode with frequency shifting by 40 MHz, using a Bragg cell. In the single component system the measurement volume had a diameter of approximately 150 μm and a length in the spanwise direction of about 1.87 mm; corresponding figures for the two component system were 146 μm and 2.19 mm, respectively.

A major technical difficulty arises when such a system is used in regions of high ambient temperature. Commercially available fibre-optic probe heads cannot be operated at temperatures above about 40 °C, because the special cements used to attach the fibre to the launching lenses become unstable. This necessitated use of a cooling jacket, which inevitably increased the diameter of the probe head (from 15 to 30 mm) and consequently increased the effects of probe blockage. Tests showed, however, that the latter remained small in the flows investigated here.

Light scattered from seed particles formed from evaporated sugar water droplets (1–3 μm nominal diameter) was collected in backscatter. To avoid introducing particle tracking errors in the LDA measurements, the seed particles must have a sufficiently high frequency response to the velocity fluctuations in the flow. Following the analysis of Drain (1980) the amplitude of the fluctuations in the velocity of the seed particles used in this study are equal to those of the fluid to within 1%, up to about 1000 Hz. This frequency response is sufficient for our purposes. The settling velocity of the seed particles is about 0.2 mm/s, which is much smaller than any velocity of interest in this study.

Burst spectrum analysers (BSA, Dantec model 57N10) were used to process the signals from the photomultiplier tubes. These processors find the Doppler frequency by Fourier transforming digitised samples of each Doppler burst. A validation test is then performed to determine the quality of the data, rejecting all samples for which the major (Doppler) spectral peak is below a factor of four larger than the next largest peak. For measurements with the single component system, the BSA was initially driven from a PC, using the commercial software provided for that purpose. Later, 'virtual instruments' were written for use with Apple Macintosh computers, using LabVIEW (a comprehensive, commercially available graphical programming language) so that, more conveniently, a single computer could be used to drive both the BSA and the cold-wire A/D board and then process the data sequences. All measurements with the two-component LDA were obtained in this way.

Measurements of temperature fluctuations were made using a DISA Type 56C01 constant temperature anemometer and a 56C20 temperature bridge with a 5 micron gold plated wire having an active length of 1.25 and 0.375 mm stubs at each end (DISA probe type 55P01). The signal was digitised using a National Instruments NB-MIO-16H acquisition board which has a 12 bit A/D converter, mounted in the Apple Macintosh computer running LabVIEW software written specifically for these measurements. The A/D converter was triggered by the burst detection system of the BSA to ensure simultaneous sampling of velocity and temperature as described below. No attempt was made to compensate for the spatial separation of the velocity and temperature measuring volumes by introducing a fixed time delay between the sampling of both (as was done by Wardana et al. 1995). Such a delay should in any case be dependent on the instantaneous velocity and it was deemed better to use a spatial separation sufficiently small to make such errors negligible (see below). Note also that in smaller scale flows a smaller diameter cold wire would be required to ensure negligible attenuation of the temperature fluctuations at high frequencies (see, for example, Tsuji et al. 1992). Tests showed, however, that in the present case this was unnecessary (see below), essentially because of the relatively large scale of the flow.

2.2
Probe arrangement

Figure 1 shows a schematic of the probe set-up. The cold-wire probe was positioned 3 mm downstream of the LDA measurement volume, with its axis parallel to the optical axis of the LDA probe. This position was chosen as a compromise between the requirement that both probes measure the same point in space and the requirement that the presence of one probe should not interfere with the other. In this case the cold-wire was found to affect the LDA measurements when the

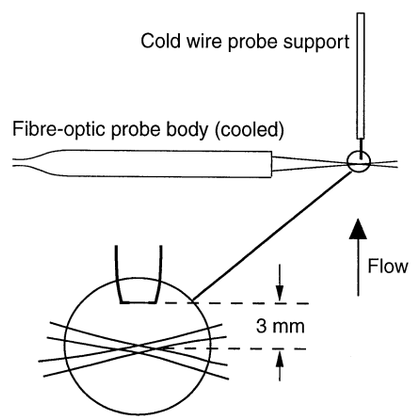

Fig. 1. Probe set-up schematic

probes were brought too close together. It was found that the best compromise was reached with a separation distance of typically 3 mm (see Sect. 3.2 below). This is significantly larger than the separation used by Wardana et al. (1995) but it should be emphasised that our flow application was of a relatively large scale. Pietri et al. (1996) found that a separation distance of about 3η, where η is the Kolmogoroff length scale, was optimum. This was a little smaller than the present separation distance and we discusss the matter further in due course.

2.3
Electronics and software

The BSA is equipped with a communications bus which is used to link it to other BSA's when multi-component LDA measurements are required. Using this bus the BSA's notify each other when the burst detection circuitry identifies a particle in the measurement volume. If all BSA's observe a burst simultaneously, the measurement will be recorded. To adapt this system to heat flux measurements careful use of the BSA's 'accept line' and 'enable line' (on the communications bus) was required, so as to ensure co-ordinated starting and sampling times for the cold wire and LDA aquisitions. Communication between the BSA and its controlling computer was required both before and after the acquisition process – to initialise the unit and to download the data, respectively – but not during it. Therefore the synchronisation of the two signals was achieved in the same way, regardless of which computer was controlling the BSA. All the data from the cold wire and the BSA(s) were recorded and, after the measurement was complete, the time series were processed to remove all those sample pairs (or triplets) which included an invalid velocity sample. In the case of the earlier measurements with the single component LDA (driven from a PC), this required transfer of the velocity time series from the PC to the Macintosh.

3
Accuracy considerations

3.1
Cold wire frequency response

Tests were performed to determine the effect of the LDA seeding on the cold-wire performance and to assess the adequacy of the wire's frequency response. Figure 2 shows temperature spectra measured before exposure to seeded flow and after the wire had been in the seeded flow for over an hour. There is virtually no difference in the two spectra and it was therefore concluded that the LDA seeding did not have an adverse affect on the sensitivity of the cold-wire in the frequency range important in the flow under consideration. It is also clear that the expected $-5/3$ region in the inertial-convective range of the temperature spectrum extends for at least a decade. This is not surprising, in view of the relatively high turbulence Reynolds number. Defining the latter in the usual way by $Re_\lambda = \lambda u'/\nu$, where λ is the Taylor microscale and u' is the rms of the axial fluctuating velocity, its value was typically 250. The exponent of the fall-off in the spectrum at lower wave-numbers agrees well with the $-17/3$ predicted by Batchelor et al. (1959), although it should be noted that there is some controversy in the literature regarding the theoretical value of the exponent.

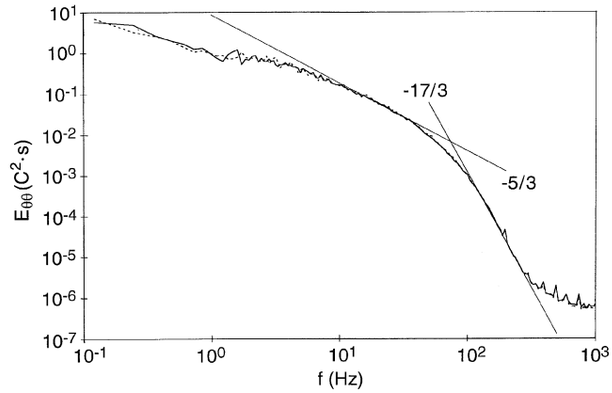

Fig. 2. Temperature spectra. The tail for $f > 300$ Hz is caused by electronic noise.

Similar measurements with a 2.5 μm diameter wire gave practically identical results, confirming that in this unusually large-scale, low velocity flow the 5 μm diameter cold wire did not suffer seriously from frequency response limitations. Use of gold-plated wires also minimised the influence of end-conduction from the prongs on the low frequency response of the probe (limiting it to the effects of the gold-plated stubs). Since the wire length (1.25 mm) was lower than the length of the LDA measurement volume (about 2 mm) spatial resolution errors in the temperature fluctuation measurements were no worse than those inherent in the velocity measurements. Errors arising from the spatial separation of the two volumes are discussed below.

3.2
Spatial resolution

As noted earlier, there is in principle some uncertainty arising from the spatial separation of the velocity and temperature measuring volumes. To validate the entire LDA-cold-wire synchronised measurement system the cold-wire was run as a hot wire so that both instruments measured the same quantity (i.e. velocity). This allowed direct comparison between the velocity-time series obtained from the two instruments. In the case of the two-component LDA this initially highlighted some synchronisation errors which would have been very difficult to identify in any other way. Once these difficulties had been overcome, time traces of velocity obtained by the hot wire and the LDA were visually coincident to a very high degree, thus giving great confidence in the hardware and software systems.

A series of measurements was made in order to determine the optimum distance between the LDA and hot/cold-wire probe. The correlation between the LDA and hot wire readings was measured for a number of separation distances and at four heights in a 1 m deep isothermal boundary layer; the results are shown in Fig. 3a. The percentage error in velocity variance as measured by the LDA caused by the presence of the hot wire probe is shown in Fig. 3b. In both figures the separation distance, Δx, has been normalised by the Kolmogoroff scale, $\eta = (\nu^3/\varepsilon)^{1/4}$. The dissipation rate, ε, was obtained by fitting the

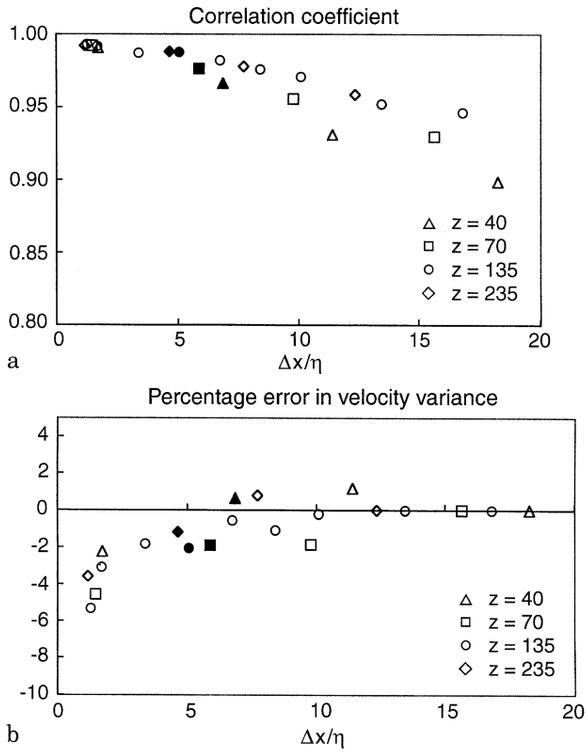

Fig. 3a, b. Effects of separation between the wire and the LDA measuring volume. z (mm): △, 40; □, 70; ○, 135; ◇, 235. Boundary layer depth is about 1 m. **a** Axial velocity correlation coefficient $-\overline{u_{hw}u_{lda}}/u'_{hw}u'_{lda}$; **b** Percentage difference in u-velocity variance

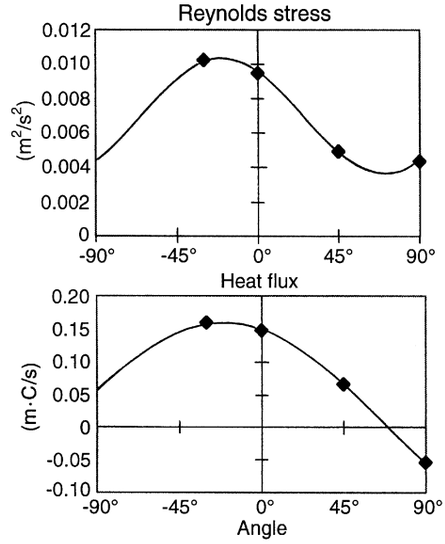

Fig. 4. Stress and flux data measured at different probe angles (α) with the single-component system, compared with the expected variations (Eqs. (1) and (2)). Stable boundary layer, at $x = 17$ m and $z = 0.075$ m

inertial subrange region of velocity spectra (measured using standard hot-wire techniques) to the universal form, with Grant et al.'s (1962) value for the subrange constant.

There is a reasonable collapse of the data for all four probe heights and, as might be expected, the correlation (Fig. 3a) falls continuously as $\Delta x/\eta$ increases. A separation of 3η or less, as suggested by Pietri et al. (1996), seems consistent with this data as the correlation coefficient remains above about 0.98 in that range. On the other hand, the effects of probe blockage (i.e. of the wire's influence on the LDA measurements) increase with decreasing separation (Fig. 3b) and at $\Delta x = 3\eta$ there is about a 2.5% error in the measured velocity variance (i.e. $\overline{u^2}$). In this work we fixed on a separation distance of 3 mm which, given that η varied between 0.44 mm (at $z = 40$ mm) and 0.65 mm (at $z = 250$ mm), corresponded to about 4–7η, depending on probe location. This implies correlation factors higher than 0.97 and variance errors less than 3%, which seemed a suitable compromise. In the stable boundary layer (Sect. 4), velocity spectra for determination of ε were not available. However, defining L_{MO} as the Monin–Obukhov length scale, estimates in the region $z < L_{MO}$ based on the size of the energy production term (and assuming dissipation = production by shear less destruction by buoyancy) yield values of η of at least 0.75 mm. It is therefore likely that in this flow a 3 mm separation distance gave errors somewhat smaller than those in the neutral flow case discussed above.

3.3 Measurement variation with probe orientation

In the measurements of a stably stratified boundary layer described below the quantities of interest were the mean longitudinal velocity, the mean temperature, three components of Reynolds stress, and the vertical heat flux. Because a one component LDA system was used initially, at least three sets of measurements were required to determine the three unknown Reynolds stresses. However, in practice four measurements were made at each point, giving a degree of redundancy in the data which could be used to test its quality. The heat fluxes and Reynolds stresses were deduced from a least-squares fitting procedure from the relations

$$\overline{u_\alpha^2} = \overline{u^2}\cos^2\alpha + \overline{w^2}\sin^2\alpha + \overline{uw}\sin 2\alpha \tag{1}$$

$$\overline{u_\alpha\theta} = \overline{u\theta}\cos\alpha + \overline{w\theta}\sin\alpha \tag{2}$$

where α is the angle between the plane containing the LDA beams and the x–y plane.

Figure 4 shows representative $\overline{u_\alpha^2}$ and $\overline{u_\alpha\theta}$ measurements obtained in the stably stratified boundary layer described in Sect. 4 and plotted as a function of α. Also shown are the best fit curves in the form of the above equations. The three unknown Reynolds stresses, $\overline{u^2}$, $\overline{w^2}$ and $\overline{uw}$, and heat fluxes, $\overline{u\theta}$ and $\overline{w\theta}$, are found from the best fit procedure. The best-fit curves fit the data very well, indicating a high degree of internal consistency in the measurements. Since the data were taken over an approximately 8 h period, these results also demonstrate that a reliably constant steady state was achieved. The two-component LDA system used subsequently did not, of course, require this approach so that measurement times were substantially lower.

4
Measurements in a stable boundary layer

4.1
Undisturbed boundary layer

Figure 5 shows measurements of mean velocity, mean temperature excess, Reynolds stresses and heat fluxes in a stably stratified boundary layer. The flow was set up in the 3.5×1.5 m cross-section wind tunnel of the Environmental Flow Research Centre in the Department of Mechanical Engineering. This facility is described by Hall (1997) and has comprehensive heating and cooling systems to allow development of a wide range of simulated atmospheric boundary layers. Detailed characterisation of non-neutral (i.e. stable or convective) flows ideally requires direct turbulence stress and heat flux measurements, since fitting *mean* velocity and temperature profiles to standard forms in order to estimate the various parameters

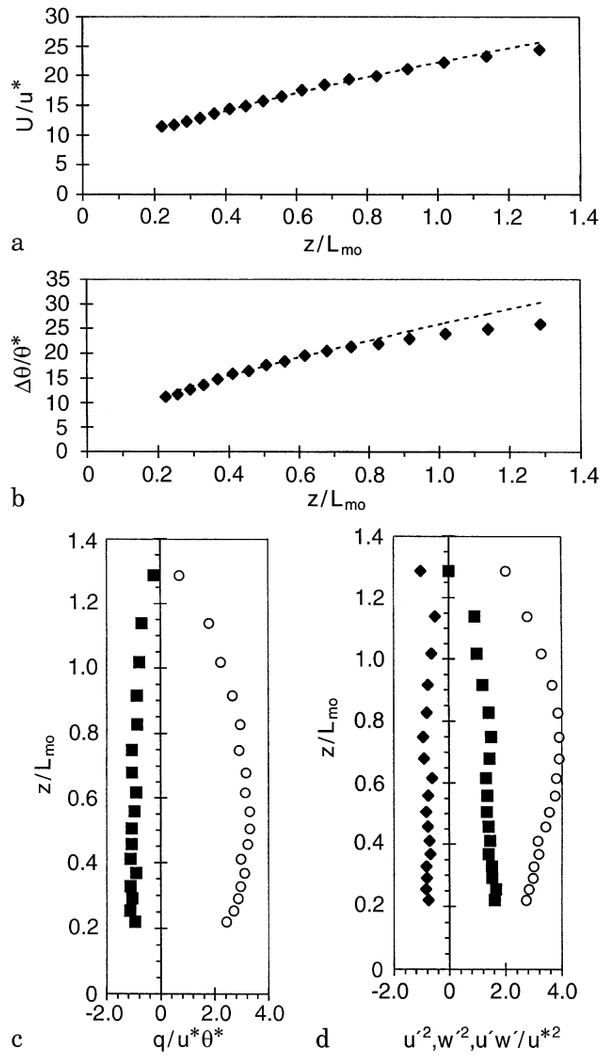

Fig. 5a–d. Profiles of mean velocity and temperature (**a**, **b**) and Reynolds stresses and heat fluxes (**c**, **d**) in the stable boundary layer at $x = 17$ m. In **a** and **b** the dotted lines are the log-linear fits of Eqs. (3) and (4), **c** ○, $\overline{u\theta}$; ■, $\overline{w\theta}$. **d** ○, $\overline{u^2}$; ■, $\overline{w^2}$; ◆, $\overline{uw}$

(surface roughness, wall friction and heat flux, etc.) is a very ill-conditioned procedure. It was this, in fact, which provided the primary motivation for development of the combined LDA-cold-wire system discussed in this paper.

For the flow used here the free-stream temperature was about 60 °C. It is the temperature difference ($\Delta\theta_0$) between the free stream and the surface which is crucial and this was held fixed at about 42 °C. All data shown here were obtained some 17 m downstream of the working section's inlet where, in addition to a barrier wall and vorticity generators (as often used for neutral boundary layer simulation), there was a set of heaters allowing the vertical inlet temperature to be profiled appropriately. At each spatial location 8000 samples were taken at a rate of approximately 20 Hz for each orientation of the LDA probe. This sampling strategy produced an uncertainty in the mean velocity of about 0.2% and in the velocity variance of about 3% with a confidence level of 95%. Detailed description of the entire flow is given in Robins et al. (1997). The data in Fig. 5 have been non-dimensionalised using the friction velocity (u^*) and the friction temperature (θ^*). These were initially estimated from the shear stress and vertical heat flux measurements ($u^* = \sqrt{-\overline{uw}}$ and $\theta^* = -\overline{w\theta}/u^*$ in the constant stress region). The curve-fits to the mean velocity and temperature profiles are of the form

$$\frac{U}{u^*} = \frac{1}{\kappa}\left[\ln\left(\frac{z}{z_0}\right) + \beta_V \frac{z}{L_{\mathrm{MO}}}\right] \tag{3}$$

and

$$\frac{\Delta\Theta}{\theta^*} = \frac{1}{\kappa}\left[\ln\left(\frac{z}{z_0}\right) + \beta_T \frac{z}{L_{\mathrm{MO}}}\right] \tag{4}$$

in standard notation. κ is von Karman's constant (0.4), z_0 is the roughness length, β_V and β_T are constants, and L_{MO} is the Monin–Obukhov length defined as:

$$L_{\mathrm{MO}} = \frac{\Theta_0 u^{*3}}{\kappa g \theta^* u^*}$$

The initial estimate of u^* was allowed to vary within the bounds of the scatter in the measurements when the fitting procedure was performed and the roughness length was constrained to lie within $\pm 20\%$ of its value in neutral conditions. The friction temperature was allowed to vary within the limits imposed by matching the normalized temperature fluctuations, $\theta_{\mathrm{rms}}/\theta^*$, to field measurements (Caughey et al. 1979) and β_V was constrained to lie between 4.0 and 5.5. The final parameter values were: $z_0 = 1.1$ mm, $u^*/u_r = 0.041$, $\theta^*/\Delta\theta = 0.032$, $L_{\mathrm{MO}} = 181$ mm, $\beta_V = 4.0$ and $\beta_T = 5.5$. It is very satisfying that the data are all internally consistent and fall centrally within the range of typical field observations (see Robins et al. 1997, where these and other data are compared with the compilation of field data presented by Hogström 1988). Without the turbulent heat flux measurements, attempts to fit the remaining data to the expected form would have led to parameter values which were much less certain.

4.2
Recirculation region behind an array of grids

As a demonstration of the true power of the LDA-cold-wire technique, velocity and heat flux measurements were performed

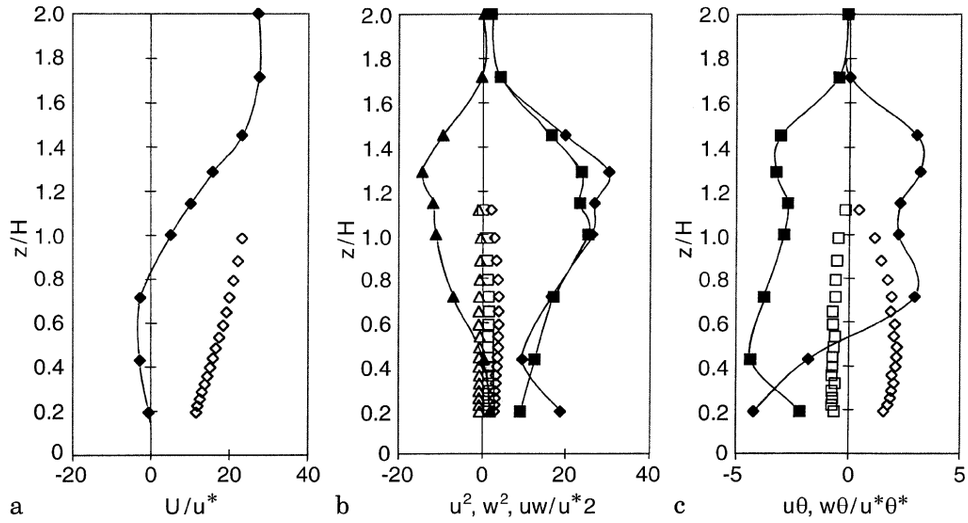

Fig. 6a–c. Measurements in the recirculation region behind porous fence array in the stable boundary layer. Open symbols are the upstream boundary layer profiles. **b** ◆, $\overline{u^2}$; ■, $\overline{w^2}$; ▲, $\overline{uw}$; **c** ◆, $\overline{u\theta}$; ■, $\overline{w\theta}$

in the recirculation region behind an array of porous grids submerged in the stable boundary layer described earlier. The array consisted of 4 steel grids (height 200 mm, length 300 mm) each with a porosity of 30%, with a 48 mm spacing between each grid in the streamwise direction. Each grid was composed of 23 vertical bars and 15 horizontal bars of cross-section 6 mm × 4 mm. There was a 10 mm gap between the floor and the bottom of the grids so that the overall height of the array, H, was 210 mm. This particular 'wake generator' was chosen for convenience – it was used in a quite separate study of flow around and through porous structures.

Figure 6 shows measurements taken 2H downstream of the last grid in the array along a vertical line centred laterally behind the grids and includes the undisturbed stable boundary layer results discussed in Sect. 4.1. The region of reverse flow near the floor can be seen clearly from the mean velocity profile. As anticipated, the Reynolds stresses far exceed their values in the undisturbed flow, reaching maxima around the location of the maximum velocity shear. Note that shear stress and the velocity gradient do not change sign at the same location (around $z/H = 0.4$ and 0.6, respectively). Note also that the longitudinal heat flux changes sign in the reverse flow region (around $z/H = 0.5$). Standard eddy viscosity models would not predict such differences between the momentum and heat flux profiles and these results therefore serve to emphasise the importance of being able to make such measurements.

5 Conclusions

A means of measuring the turbulent heat flux using combined LDA and cold-wire anemometry systems has been described. We have shown that such an approach can be used even in large scale flows of relatively high temperature. The former requires use of fibre optics for the light delivery and the latter necessitates use of probe-head cooling. Single or twin computers can be used to drive the LDA's Burst Spectrum Analysers and the cold-wire circuitry for simultaneous measurement of fluctuating velocity and temperature, respectively. With distances between the cold wire and the LDA measuring volume below about seven Kolmogoroff length scales, the joint effects of spatial separation and blockage of the cold wire are found to be small. Finally, measurements in a thick stable boundary layer have been used to demonstrate the power of the technique and it is concluded that the potential of such an approach is considerable, particularly as there are no limitations imposed by high turbulence intensity and instantaneous flow reversals.

References

Antonia RA; Danh HQ; Prabhu A (1977) Response of a turbulent boundary layer to a step change in surface heat flux. J Fluid Mech 80: 153–177

Antonia RA; Krishnamoorthy LV; Fulachier L (1988) Correlation between the longitudinal velocity fluctuation and temperature fluctuation in the near-wall region of a turbulent boundary layer. Int J Heat Mass Trans 31: 723–730

Batchelor GK; Howells ID; Townsend AA (1959) Small-scale variation of convected quantities like temperature in turbulent fluid. Part 2. The case of large conductivity. J Fluid Mech 5: 134–139

Bruun HH (1995) Hot Wire Anemometry. Oxford University Press, London

Caughey SJ; Wyngaard JC; Kaimal JC (1979) Turbulence in the evolving stable boundary layer. J Atmos Sci 36: 1041–1052

Drain LE (1980) The Laser Doppler Technique. J. Wiley

Gibson CH (1968) Fine structure of scalar fields mixed by turbulence. II, spectral theory. Phys Fluids 11: 2316–2327

Gibson MM; Verriopoulos CA (1984) Turbulent boundary layers on a mildly curved convex surface 2. Temperature field measurements. Exp Fluids 2: 73–80

Grant HL; Stewart RW; Molliet A (1962) Turbulence spectra from a tidal channel. J Fluid Mech 12: 241–268

Hall RC (ed) (1992) Evaluation of modelling uncertainty, EC Report, Contract number EV5V-CT94-0531

Hishida M; Nagano Y (1979) Structure of turbulent velocity and temperature fluctuations in fully developed pipe flow. J Heat Trans 101: 15–22

Högström U (1988) Non-dimensional wind and temperature profiles in the atmospheric surface layer: a re-evaluation. Bound Layer Meteor 42: 55–78

Lienhard JHV (1988) Decaying turbulence in thermally stratified flow, PhD thesis. University of California at San Diego

Pietri L; Djeridane T; Amielh M; Fulachier L (1996) Simultaneous measurements of temperature and velocity combining cold wire and laser doppler velocimetry in a slightly heated turbulent jet. Advances in Turbulence VI, 523–524. S. Gavilakis et al. (eds), Kluwer

Robins AG; Heist D; Hayden P; Tyson I (1997) Simulation of moderately stable atmospheric boundary layers in a wind tunnel, In preparation

Thole KA; Bogard BG (1994) Simultaneous temperature and velocity measurements. Meas Sci Technol 5: 435–439

Tsuji T; Nagano Y; Tagawa M (1992) Frequency response and instantaneous temperature profile of cold-wire sensors for fluid temperature fluctuation measurements. Exp Fluids 13: 171–178

Wardana ING; Ueda T; Mizomoto M (1995) Velocity-temperature correlation in strongly heated channel flow. Exp Fluids 18: 454–461